Lifetime of the 1.04 MeV state in ^{18}F, measured through the inverse reaction ^{3}He(^{16}O, p)^{18}F

J. Keinonen and H.-B. Mak
Department of Physics, Queen's University, Kingston, Ontario, Canada K7L 3N6

T. K. Alexander, G. C. Ball, W. G. Davies, J. S. Forster, and I. V. Mitchell
Atomic Energy of Canada Limited, Chalk River Nuclear Laboratories, Chalk River, Ontario, Canada K0J 1J0

(Received 12 November 1980)

The mean lifetime of the 1.04 MeV ($J^{\pi} = 0^{+}, T = 1$) state in ^{18}F has been measured to be 2.7 ± 0.7 fs using the inverse reaction ^{3}He(^{16}O,p)^{18}F and the Doppler-shift attenuation method. Targets of ^{3}He implanted into Al, Zr, Nb, and Au foils were employed in the measurements. The centroid shifts and Doppler-broadened line shapes observed at 0° were used in obtaining the lifetime value. The lifetime of the 1.04 MeV state is compared with theoretical predictions.

[NUCLEAR REACTIONS ^{3}He(^{16}O, p)^{18}F, $E = 15.9$ MeV; measured Doppler-shift attenuation, $p\gamma$ coin. ^{18}F 1.04 MeV level deduced τ.]

I. INTRODUCTION

The 1.08 ($J^{\pi} = 0^{-}, T = 0$) and 1.04 ($0^{+}, 1$) MeV states in ^{18}F provide a favorable system to study the $\Delta T = 1$ component of the parity mixing in nuclear wave functions. Recent studies[1,2] of the circular polarization of the $E1$ transition 1.08 ($0^{-}, 0$) $\rightarrow 0(1^{+}, 0)$ MeV have prompted attempts to improve the experimental lifetime value of the 1.04 MeV level needed in the deduction of the parity-nonconserving (PNC) nucleon-nucleon interaction. In a recent experiment[3] the value was measured to be $\tau = 2.7^{+0.6}_{-0.4}$ fs.

Previous Doppler shift attenuation (DSA) measurements were made at low initial velocity through the ^{18}O(p,n)^{18}F resonance at $E_p = 3.75$ MeV. Our aim in the present work was to obtain confirmation of the lifetime by measuring it under experimental conditions where the deduced value is subject to different systematic errors. The very recent experimental data[4] on the density changes of helium implanted targets provide a basis for extending the use of the inverse reaction ^{3}He(^{16}O,p)^{18}F to the DSA measurement of this extremely short lifetime.

II. EXPERIMENT AND RESULTS

The apparatus and general experimental procedure were the same as those described in Refs. 4–6. A beam of 15.90 MeV ^{16}O^{3+} ions from the Chalk River MP Tandem accelerator was used to bombard thin metallic foils of Al, Zr, Nb, and Au implanted with 35 keV ^{3}He ions from the Chalk River 70 kV isotope separator. Characteristics of the targets are summarized in Table I. The target foils were thick enough to stop both the oxygen beam and ^{18}F recoils from the ^{3}He(^{16}O,p)^{18}F reaction. Protons were detected and identified in a ΔE-E telescope consisting of 50 μm and 1 mm thick surface barrier counters positioned at 0° to the beam direction, the half angle subtended by the proton counter being 14°. The corresponding ^{18}F ions recoiled with an average initial velocity of about 0.034 the velocity of light in a narrow cone of half-angle 2.7°.

Although the proton groups from the 0.94, 1.04, and 1.08 MeV states could not be resolved, the proton energy resolution was adequate to ensure only direct feeding of the 1.04 MeV level. The Doppler shifted 1042 keV γ rays were detected in a 100 cm^{3} Ge(Li) detector at 0°. The detector was located 8.0 cm from the target and was shielded from low energy γ rays and x rays by 1 mm of lead. This detector was gain stabilized by taking $\gamma\gamma$ coincidences from ^{88}Y and ^{60}Co sources with a second Ge(Li) detector which was shielded from the target by 10 cm of lead. The $\gamma\gamma$ coincidences from the ^{60}Co source were also used to generate a γ-ray line shape at 1173 keV for the DSA analysis. All $p\gamma$- and $\gamma\gamma$-coincidence data were recorded event by event on magnetic tape and played back later on the PDP-10 computer.

To find the optimum yield for the 1042 keV γ rays in the DSA measurements, the excitation function of the ^{16}O(^{3}He,p)^{18}F reaction was measured from $E_{^{3}\mathrm{He}} = 2.80$ to 3.75 MeV. The ^{3}He beam from the Queen's University 4 MV Van de Graaff accelerator was used to bombard a differentially pumped ^{16}O gas target[13] maintained at 26.6 Pa (0.2 Torr) pressure. Based on the proton energy spectra recorded at 150°, a suitable population of the 1.04 MeV state was found at $E_{^{3}\mathrm{He}} \sim 2.9$ MeV, through a group of overlapping resonances with a sharp front edge (45 keV).

TABLE I. Characteristics of the implanted ^{3}He targets and the summary of lifetime analysis of the ^{18}F, 1.04 MeV level.

Target[a]	Dose[b] (10^{21} atoms/m^2)	σ[c] (μm)	α_N^{-1}[d] (ps^{-1})	χ^2	τ (fs)[e]
Au(3)	3.1	0.05	3.03	1.4	3.8 ± 1.4(0.7)
Au(4)	4.0	0.05	3.03	0.8	5.2 ± 1.2(0.8)
Nb(7)	7.0	0.06	2.37	1.1	$3.5^{+1.7(+1.1)}_{-3.5(-3.5)}$
				1.5	<2.4(<2.0)
Zr(4)	4.0	0.07	1.79	2.0	<3.0(<2.6)
Al(4)	4.1	0.10	1.18	1.3	<3.5(<3.2)
Average (summed χ^2)				1.6	3.5 ± 1.0(0.5)
Centroid shift analysis				0.7	2.0 ± 0.9(0.7)[f]
Average					2.7 ± 0.7

[a] The numbers in parentheses refer to the ^{3}He dose and are used to label the targets.

[b] The implanted area was 1 cm^2. Nuclear microanalysis through the ^{3}He$(d,p)^4$He reaction showed that the retained ^{3}He and the ^{3}He fluences were linearly related for all targets and that the implant dose was uniform across each target.

[c] Adopted ^{3}He profile standard deviations from Refs. 7–9.

[d] The slowing down parameter for ^{18}F at $v = 0.034c$ in the unimplanted material is calculated from the stopping powers of Refs. 10 and 11 using the modification outlined in Ref. 12.

[e] Values in parentheses are statistical errors only. Total errors include uncertainty in the recoil velocity distribution, the counter response function, the stopping power, and the implanted target density. All limits are given with 1σ confidence level.

[f] Value in brackets is the statistical error only. The total error includes uncertainty in the average recoil velocity, the stopping power, and the target density.

A thin target yield curve is shown in Fig. 1(d) where the ^{3}He bombarding energy scale has been multiplied by 5.3034 (the ratio of the mass of ^{16}O to ^{3}He) to give an equivalent ^{16}O bombarding energy. Also shown in Figs. 1(a), 1(b), and 1(c) are the yield curves for the Au(3), Nb(7), and Al(4) targets (see Table I) measured for the coincidence 1042 keV γ rays from the ^{3}He$(^{16}$O$,p\gamma)^{18}$F reaction. The dashed curve in Fig. 1(a) is the yield of the 1081-keV coincident γ rays. The 1042 keV gamma ray yield curves for the different targets are nearly identical in shape and the peak positions are the same within 15 keV. The solid lines are fits to the data with the range and width of the ^{3}He depth distribution as parameters. The widths of the depth distribution of ^{3}He targets deduced from these yield curves and the cross-section data shown in Fig. 1(d) are 510 ± 80 keV full width at half maximum (FWHM) ($\sigma = 0.11 \pm 0.02$ μm), 600 ± 100 keV ($\sigma = 0.068 \pm 0.01$ μm) and 530 ± 110 keV ($\sigma = 0.044 \pm 0.01$ μm) for the Al, Nb, and Au targets, respectively. These values confirm the standard deviations of the ^{3}He depth distributions given in Table I, which were used in the lifetime analysis.

Figure 1(e) shows the relative positions of the ^{3}He depth distribution in the Al(4) target for $E_{^{16}O} = 15.9$ MeV and the cross section for the reaction [Fig. 1(d)]. Figure 1(f) is the product of these two functions and shows the average effective bombarding energy to be 15.540 MeV with a full width at half maximum 420 keV. The average value of the effective bombarding energy for all targets is 15.56 ± 0.02 MeV.

Line shape data from each target were accumulated over 16 to 24 h bombardment periods at an average beam current of about 150 nA of ^{16}O^{3+}. Figure 2 shows parts of the coincident γ-ray spectra in the region of the Doppler shifted 1042 keV full energy peak for the Au(3) and Al(4) targets; random coincidences and background have been subtracted. The low energy Compton tails of the 1081 and 1042 keV photopeaks were removed by using a spectrum stripping procedure[5] and the shape of the 1173 keV ^{60}Co line generated in the $\gamma\gamma$-coincidence spectrum. The lifetime of the 1.04 MeV state was determined from both the centroids and the lineshapes of the Doppler-shifted 1042 keV γ-ray peaks. The results are summarized in Table I.

The centroids of the 1081 keV γ ray and the Doppler shifted 1042 keV γ-ray peaks are displayed in Fig. 3. The centroids of the 1081 keV peak were obtained by fitting the stripped 1173 keV ^{60}Co line to the peak. The consistency of these data provided an excellent test for relative systematic errors. The absolute weighted average γ-ray energy of 1080.58 ± 0.04 keV corresponds to an excitation energy of 1080.61 ± 0.04 keV, in good agreement with the literature value[14]

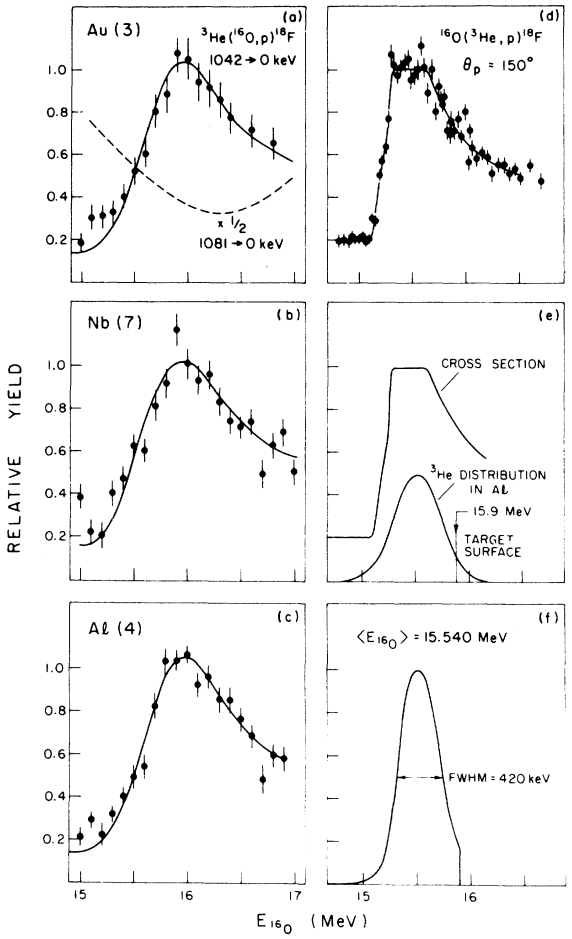

FIG. 1. Excitation functions of the coincident 1042 keV γ rays from the ^{3}He(^{16}O, p)^{18}F reaction are shown in (a), (b), and (c) for the targets indicated. The dashed curve in (a) is the yield curve for the 1081 keV coincident γ rays. (d) is the thin target yield curve for the ^{16}O(^{3}He, p)^{18}F reaction; the energy scale is converted to equivalent ^{16}O energy. (e) shows a smoothed representation of (d) and a depth distribution of ^{3}He in Al positioned relative to the bombarding energy 15.9 MeV. (f) is their product and gives the yield as a function of the beam energy in the target for a bombarding energy of 15.9 MeV.

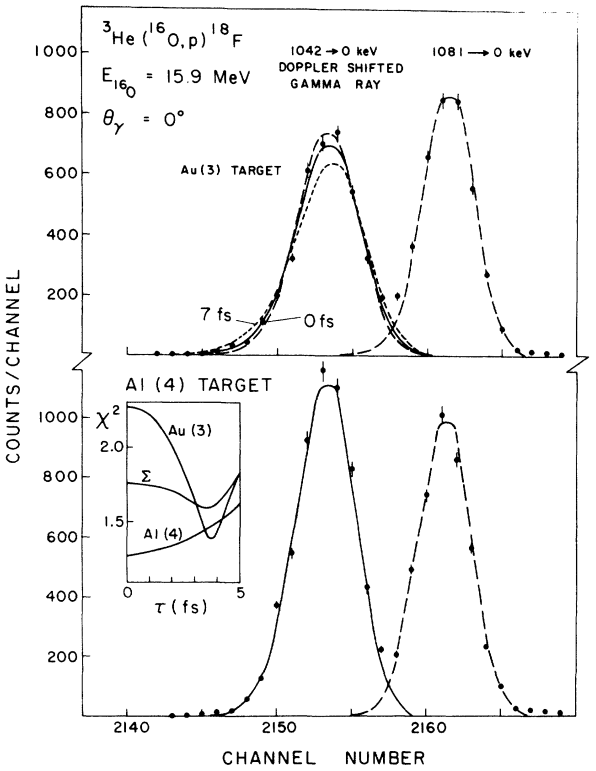

FIG. 2. Doppler broadened γ-ray line shapes in the Au(3) (top) and Al(4) (bottom) targets for the 1.04 → 0 MeV transition in ^{18}F. The energy dispersion is 0.50 keV/channel. Background and the counts from the Compton distribution of the 1042 and 1081 keV γ rays have been subtracted. See the text. The solid lines are the best fits to the line shapes for the lifetime values shown by minima of the χ^2 plot in the inset. The theoretical line shapes shown by dashed lines for the Au(3) target illustrate the sensitivity to the mean life τ of the 1.04 MeV level. In order to emphasize the changes in the line shape, the centroids have been adjusted to the same value. The instrinsic line shapes used for calculating and fitting both the 1042 and 1081 keV line shapes were the experimental 1173 keV line shapes from the ^{60}Co source shown as dashed curves for the 1081 → 0 keV peaks. The curve Σ in the inset illustrates the sum of all χ^2 plots listed in Table I.

of 1080.54 ± 0.12 keV. The error limits have been increased to include an uncertainty in the linearity of the electronics. The centroids of the Doppler shifted 1042 keV γ-ray peak were obtained directly from the intensity distributions after correcting for the tail of the fitted 1081 keV γ-ray line.

For short lifetimes measured in a homogeneous medium, the average γ-ray energy observed at 0° is related to the mean lifetime by the expression[15]

$$\langle E_\gamma \rangle = E_\gamma(t=0) - \Delta E_\gamma \alpha_N^{-1} \tau \,, \qquad (1)$$

where $E_\gamma(t=0)$ is the fully shifted γ-ray energy, ΔE_γ is the full Doppler shift and $\alpha_N^{-1} = (1/v)(dv/dt)$ is the characteristic slowing down time of the material. For an implanted target the characteristic slowing down time in the region of swollen material is given by[4]

$$\alpha^{-1} = \alpha_N^{-1} \frac{1+\delta}{1+Ac} \,,$$

where c is the local atomic concentration of ^{3}He, A is a material dependent proportionality constant, and $1+\delta$ is the correction factor to the stopping power for the added ^{3}He.

In the present analysis the targets were approximated by a two-layer medium in which the Gaussian implant profiles with peak concentration C_0 and standard deviations σ were taken to be rectangular profiles with a width of $\sqrt{2\pi}\sigma$. The corresponding effective slowing down parameters α_{eff}^{-1} were determined by using the experimental value[4] $A = 0.75 \pm 0.25$ and the two-layer formula given in Ref. 4. After replacing α_N^{-1} by α_{eff}^{-1} in Eq. (1), the least-squares fit of the equation to the data shown in Fig. 3(b) yielded the value $\tau = 2.0 \pm 0.7$ fs. From the measured intercept [$E_\gamma(t=0) = 1076.67 \pm 0.04$ keV], the calculated full shift ΔE_γ and nuclear recoil energy, the level energy 1041.58 ± 0.08 keV was obtained for the second excited state in ^{18}F. This is in good agreement with the literature value[14] of 1041.55 ± 0.08 keV and with the values of 1041.52 ± 0.06 keV and 1041.51 ± 0.02 keV obtained from a reevaluation of the data in a recent experiment.[3] The first value was obtained from the average of two γ-ray energy measurements at 90° and the second from a centroid shift analysis of 0° data.

The experimental Doppler broadened γ-ray lineshapes were analyzed as described in Refs. 5 and 6, and lifetimes were deduced by comparing experimental line shapes with those calculated with the same experimental stopping powers as used in the centroid shift analysis. The calculated line shape took into account the initial velocity distribution of the ^{18}F ions, the γ-ray detector response function, and the swelling of the target layer. Representative best fits are shown as solid lines in Fig. 2 and a summary of results is given in Table I. The different targets yielded consistent values. A weighted average $\tau = 3.5 \pm 1.0$ fs was obtained from a sum of the χ^2 plots, shown by Σ in the inset of Fig. 2. The result of the line shape analysis is in agreement with the value $\tau = 2.0 \pm 0.9$ fs obtained from the centroid analysis and the weighted average is 2.7 ± 0.7 fs.

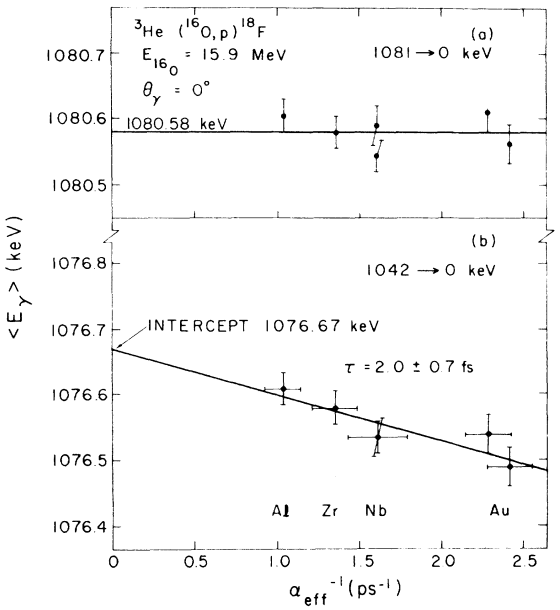

FIG. 3. (a) The centroid energies, obtained with the different targets, for the 1081 keV γ-ray line [τ(1.08 MeV) = 27.5 ± 1.19 ps (Ref. 14)]. (b) The centroid energy of the Doppler-shifted 1.04 → 0 MeV transition is shown as a function of inverse stopping time α_{eff}^{-1} for the targets listed in Table I. The solid line is the least squares fit of Eq. (1) to the experimental points.

III. DISCUSSION

This measurement represents the first application of high velocity DSAM and implanted targets to determine such short lifetimes. The accuracy is limited by uncertainties in the properties of the implanted ^{3}He targets and our ability to determine centroids accurately. The latter can always be improved by better counting statistics. However, the former requires further investigation since uncertainties in the depth profiles of the targets result in uncertainties for the effective bombarding energy differences between the different targets (±20 keV in the present work). In addition, details of the swelling ($\Delta A/A = 0.3$ and $\Delta\sigma/\sigma = 0.2$ in the present work) and other changes in the structure of the material limit the accuracy to which α_{eff}^{-1} is known. These uncertainties are shown as horizontal error bars in Fig. 3. The values for α_N^{-1} given in Table I have uncertainties of 5% for the Au targets. Errors of 10% have been allowed for Zr, Nb, and Al because their values involve more interpolation. However, in a separate experiment[16] the lifetime ($\tau \sim 1$ ps) of the 1.70 MeV level of ^{18}F was measured by using the Au, Nb, and Al targets and the values deduced agreed within 5%. This confirms the consistency of the stopping powers used in the present analysis.

By combining the present value with the reanalyzed value of 4 ± 2 fs from Ref. 17 (see Ref. 3) and with the recent value[3] of $2.7^{+0.6}_{-0.4}$ fs, a weighted average $\tau(1.04\ \text{MeV}) = 2.7 \pm 0.4$ fs is obtained.

The circular polarization $P_\gamma(1.08\ \text{MeV})$ is given by[18]

$$P_\gamma(1.08\ \text{MeV}) = -2\frac{\langle 1.04(0^+,1)|V^{\text{PNC}}|1.08(0^-,0)\rangle\langle 0(1^+,0)||M1||1.04(0^+,1)\rangle}{\Delta E\langle 0(1^+,0)||E1||1.08(0^-,0)\rangle},$$

where $\langle|V^{PNC}|\rangle$ is the PNC matrix element, ΔE = 39 keV the energy difference between the mixed states, and $\langle\|M\|\rangle$ and $\langle\|E1\|\rangle$ the reduced matrix elements of the $M1$ and $E1$ transitions 1.04 → 0 MeV and 1.08 → 0 MeV, respectively. Using the $M1$ strength derived from the weighted mean τ above, $|M|^2 = 10.3 \pm 1.5$ W.u., and the $E1$ strength[14] $(4.1 \pm 0.3) \times 10^{-3}$ W.u. of the 1.08 MeV $(0^-, 0) \rightarrow 0$ MeV $(1^+, 0)$ transition, $P_\gamma(1.08\ \text{MeV}) = \pm(5.8 \pm 0.4)$ keV^{-1} $\langle 1.04(0^+, 1)|V^{PNC}|1.08(0^-, 0)\rangle$. The experimental circular polarization values, $P_\gamma(1.08) = (-0.7 \pm 2.0) \times 10^{-3}$ (Ref. 1) and $(-0.9 \pm 1.7) \times 10^{-3}$ (Ref. 2), give an average value $P_\gamma(1.08) = (-0.8 \pm 1.3) \times 10^{-3}$. The predictions of Gari *et al.*,[18] would be increased by a factor of 1.20 if the present values for the transition strengths and energy separation were used. In the Cabibbo-model prediction of Ref. 18, this implies an "enhancement factor" produced by neutral weak currents of less than 8 (2σ limit), depending on the sign of the predicted value. More recent discussions of the theoretical interpretation of measurements on parity violations in nuclei can be found in Refs. 19, 20, and 21.

It is a pleasure to thank R.L. Brown for technical assistance, O.M. Westcott for implanting the targets with ^{3}He, and N. Burn and his staff for operating the MP tandem.

[1] C. A. Barnes, M. M. Lowry, J. M. Davidson, R. E. Marrs, F. B. Morinigo, B. Chang, E. G. Adelberger, and H. E. Swanson, Phys. Rev. Lett. 40, 840 (1978).
[2] G. Ahrens, thesis, Mainz, 1980 (unpublished). The sign convention quoted here is the same as that used in Ref. 1. (Private communication from H. Schober, Mainz University, Mainz).
[3] J. Keinonen, H. B. Mak, P. Skensved, J. R. Leslie, and W. McLatchie, Phys. Rev. C 22, 351 (1980).
[4] T. K. Alexander, G. C. Ball, W. G. Davies, and I. V. Mitchell, J. Nucl. Mat. 96, 51 (1981).
[5] J. S. Forster, T. K. Alexander, G. C. Ball, W. G. Davies, I. V. Mitchell, and K. B. Winterbon, Nucl. Phys. A313, 397 (1979).
[6] T. K. Alexander, G. C. Ball, W. G. Davies, and J. S. Forster, Nucl. Phys. A313, 425 (1979).
[7] J. F. Ziegler, *Helium: Stopping Powers and Ranges in All Elemental Matter* (Pergamon, New York, 1977).
[8] R. Behrisch, J. Bottiger, W. Eckstein, U. Littmark, J. Rothand, and B. M. U. Scherzer, Appl. Phys. Lett. 27, 199 (1975).
[9] J. Bottiger, P. S. Jensen, and U. Littmark, J. Appl. Phys. 49, 965 (1978).
[10] J. S. Forster, D. Ward, H. R. Andrews, G. C. Ball, G. J. Costa, W. G. Davies, and I. V. Mitchell, Nucl. Instrum. Methods 136, 349 (1976).
[11] L. C. Northcliffe and R. F. Schilling, Nucl. Data Tables 7, 233 (1970).
[12] D. Ward, J. S. Forster, H. R. Andrews, I. V. Mitchell, G. C. Ball, W. G. Davies, and G. J. Costa, Atomic Energy of Canada Ltd. Report No. AECL-5313, 1976.
[13] H. C. Evans, Annual Report, 1979, Queen's University, Kingston (unpublished).
[14] F. Ajzenberg-Selove, Nucl. Phys. A300, 1 (1978).
[15] E. K. Warburton, J. W. Olness, and C. J. Lister, Phys. Rev. C 20, 619 (1979).
[16] J. Keinonen, H. B. Mak, T. K. Alexander, G. C. Ball, W. G. Davies, J. S. Forster, and I. V. Mitchell (unpublished).
[17] A. E. Blaugrund, D. N. Youngblood, G. S. Morrison, and R. E. Segel, Phys. Rev. 158, 893 (1967).
[18] M. Gari, J. B. McGrory, and R. Offermann, Phys. Lett. 55B, 277 (1975).
[19] D. Tadic, Rep. Prog. Phys. 43, 67 (1980).
[20] B. A. Brown, W. A. Richter, and N. S. Goodwin, Phys. Rev. Lett. 45, 1681 (1980).
[21] W. C. Haxton, B. F. Gibson, and E. M. Henley, Phys. Rev. Lett. 45, 1677 (1980).